

Figure S1. Nucleotide hamming distance to nearest neighbor distribution plots of B cell receptor junctional sequences. The distributions are bimodal in DLN and spleen samples with a red dashed line located at a distance of 0.06 separating the two modes plotted. DLN, tumor draining lymph node; mDX400, murine anti-PD-1; mIgG1, murine immunoglobulin G1.

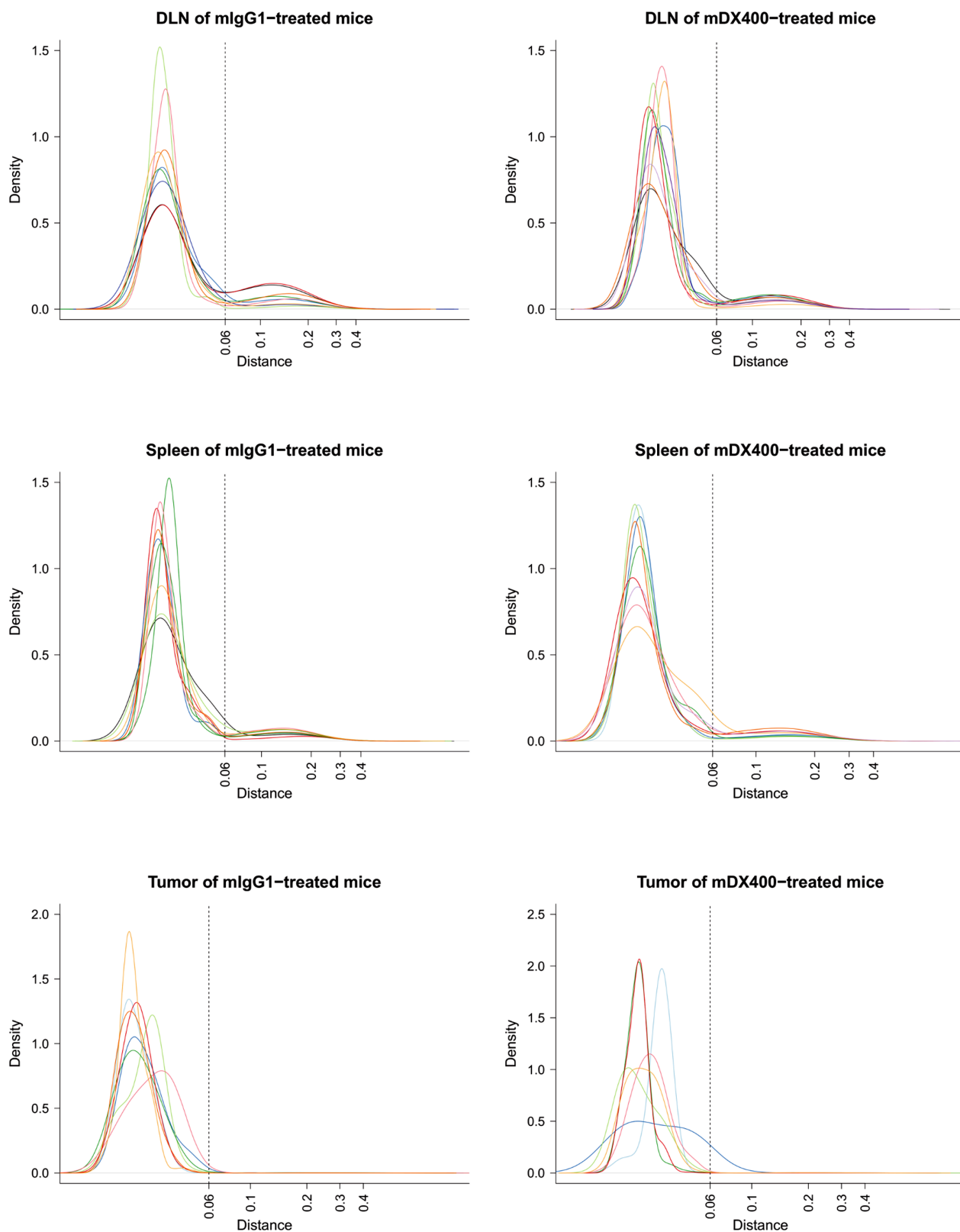


Figure S2. Frequencies of the top 10 most frequent T cell receptor clonotypes in murine anti-PD-1-group tumor samples. A horizontal dashed red line marks the frequency of 0.1%, which was also plotted.

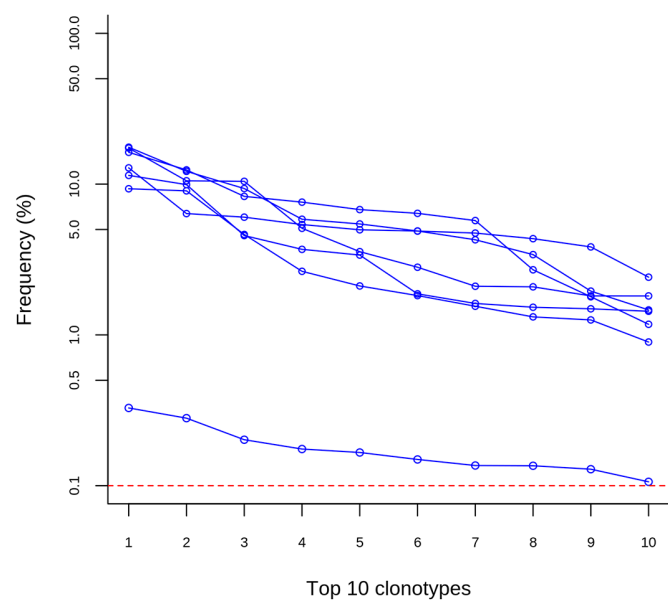
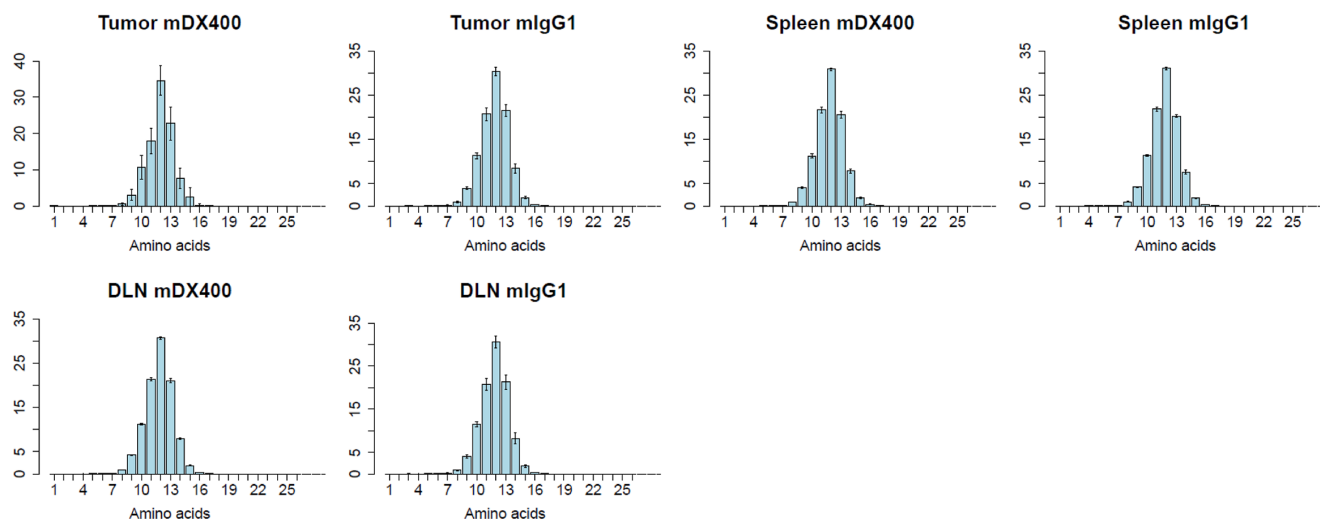


Figure S3. Length distribution of TCR/BCR CDR3 amino acid sequences. Length distribution was plotted for tumor, spleen and DLN samples from mDX400- and mIgG1-treated groups. Data are represented as the mean  $\pm$  standard deviation. TCR, T cell receptor; BCR, B cell receptor; CDR3, complementarity determining region 3; DLN, tumor draining lymph node; mDX400, murine anti-PD-1; mIgG1, murine immunoglobulin G1.

### CDR3 amino acid sequence length of TCR



### CDR3 amino acid sequence length of BCR

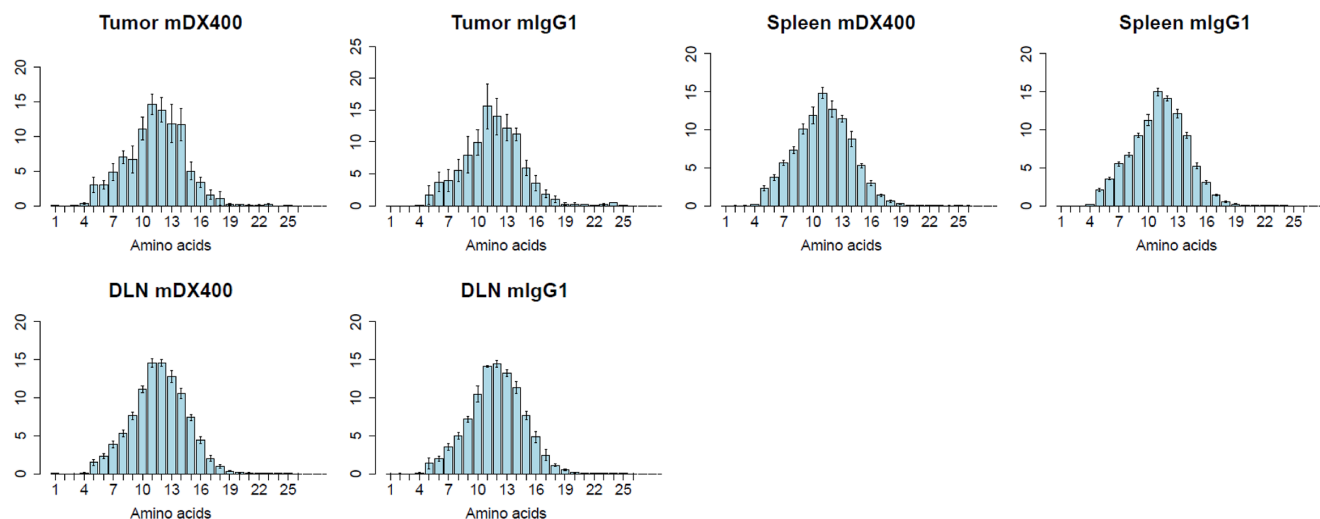


Figure S4. Hill diversity profiles of TCR repertoires in spleen and DLN samples. mDX400- and mIgG1-group samples are depicted in blue and red, respectively. The diversity profile of each group was represented by a set of boxplots with each boxplot displaying the diversity values in  ${}^qD$  relative to a certain  $q$ . The  $q$  values ranging from 0 to 10 in 0.1 increments are shown on the plot. TCR, T cell receptor; DLN, tumor draining lymph node; mDX400, murine anti-PD-1; mIgG1, murine immunoglobulin G1.

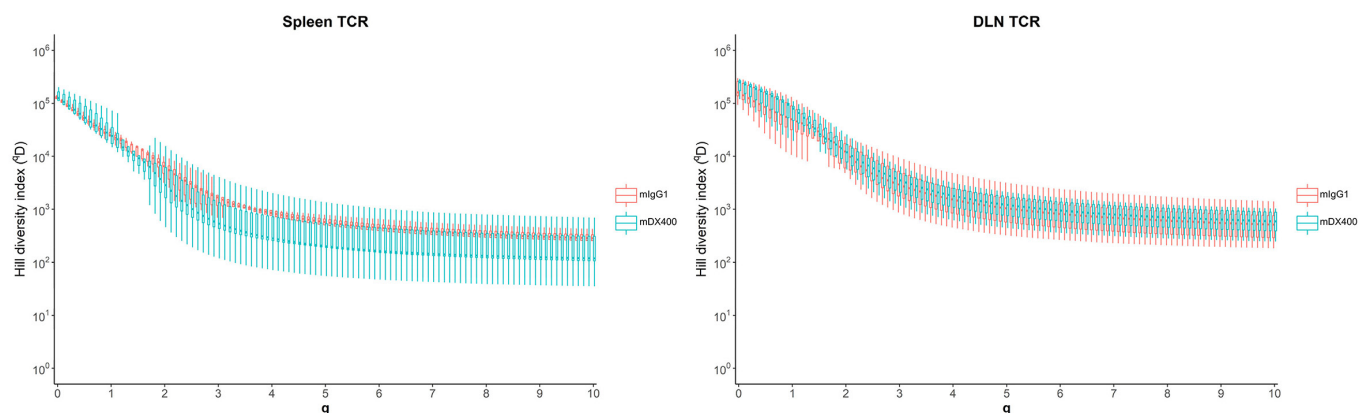


Figure S5. Selection strength in the CDR2 and FWR3 of BCR repertoires. Each curve illustrates the posterior probability distribution of the selection strength for BCR sequences from tumor, spleen and DLN samples. mDX400- and mIgG1-group samples are depicted in blue and red, respectively. CDR2, complementarity determining region 2; FWR3, framework region 3; BCR, B cell receptor; DLN, tumor draining lymph node; mDX400, murine anti-PD-1; mIgG1, murine immunoglobulin G1.

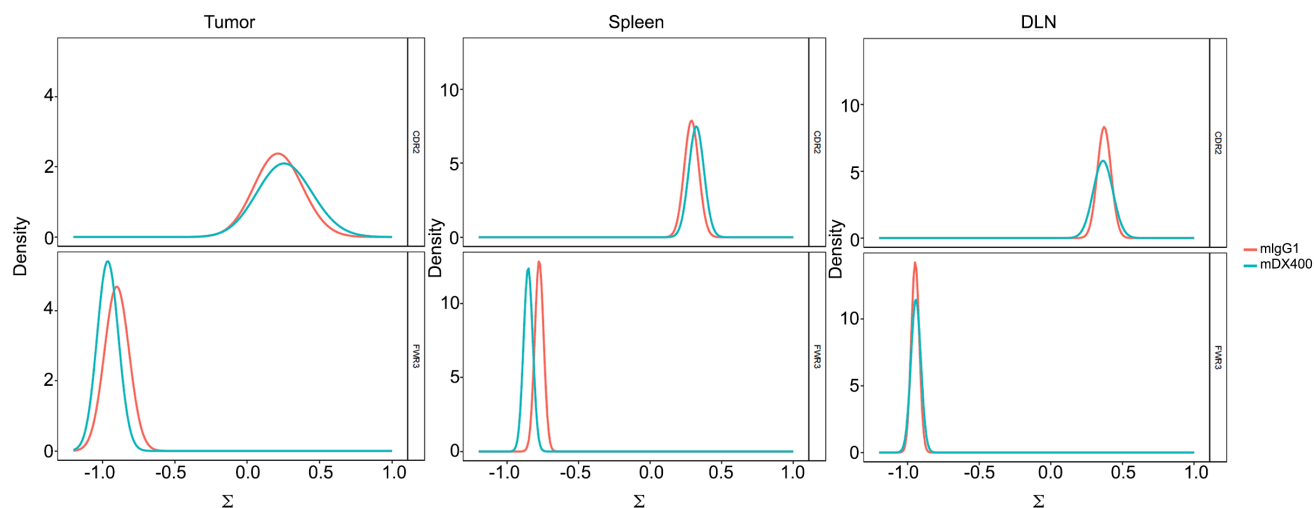


Figure S6. Mutation rates of intratumoral immunoglobulin heavy chain repertoires. Mutation rates are represented by the number of mutant bases per  $10^4$  base pairs within CDR2 and FWR3, separately and together. mDX400- and mIgG1-group tumor samples are depicted in blue and red, respectively. Data are represented as the mean  $\pm$  standard deviation. CDR2, complementarity determining region 2; FWR3, framework region 3; mDX400, murine anti-PD-1; mIgG1, murine immunoglobulin G1.

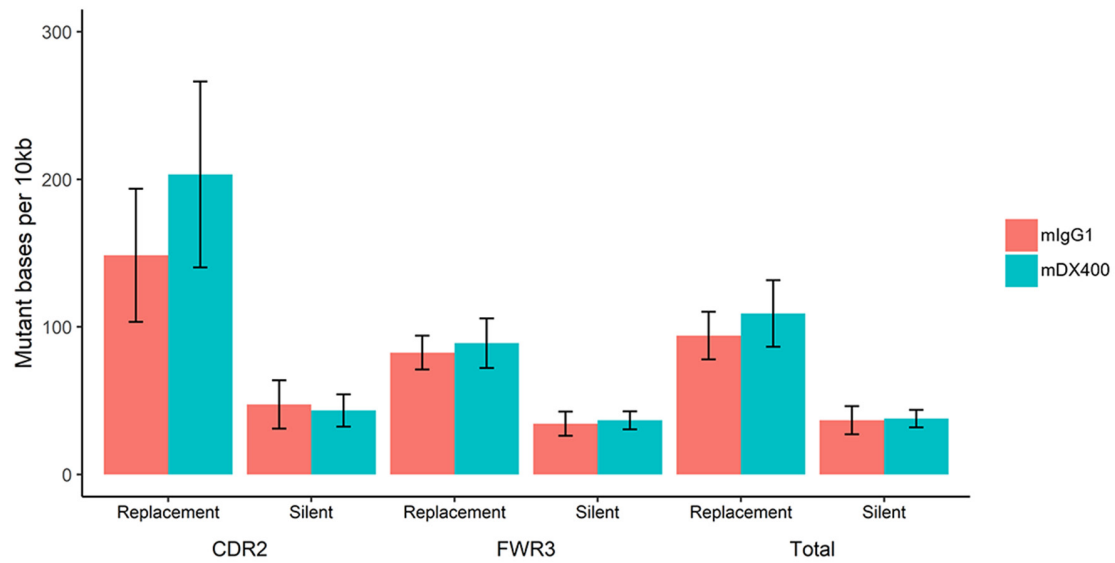


Figure S7. Hill diversity profiles of BCR repertoires in tumor, spleen and DLN samples. mDX400- and mIgG1-group samples are depicted in blue and red, respectively. The diversity profile of each group is represented by a set of boxplots with each boxplot displaying the diversity values in  $^qD$  relative to a certain  $q$ . The  $q$  values ranging from 0 to 10 in 0.1 increments are shown on the plot. BCR, B cell receptor; DLN, tumor draining lymph node; mDX400, murine anti-PD-1; mIgG1, murine immunoglobulin G1.

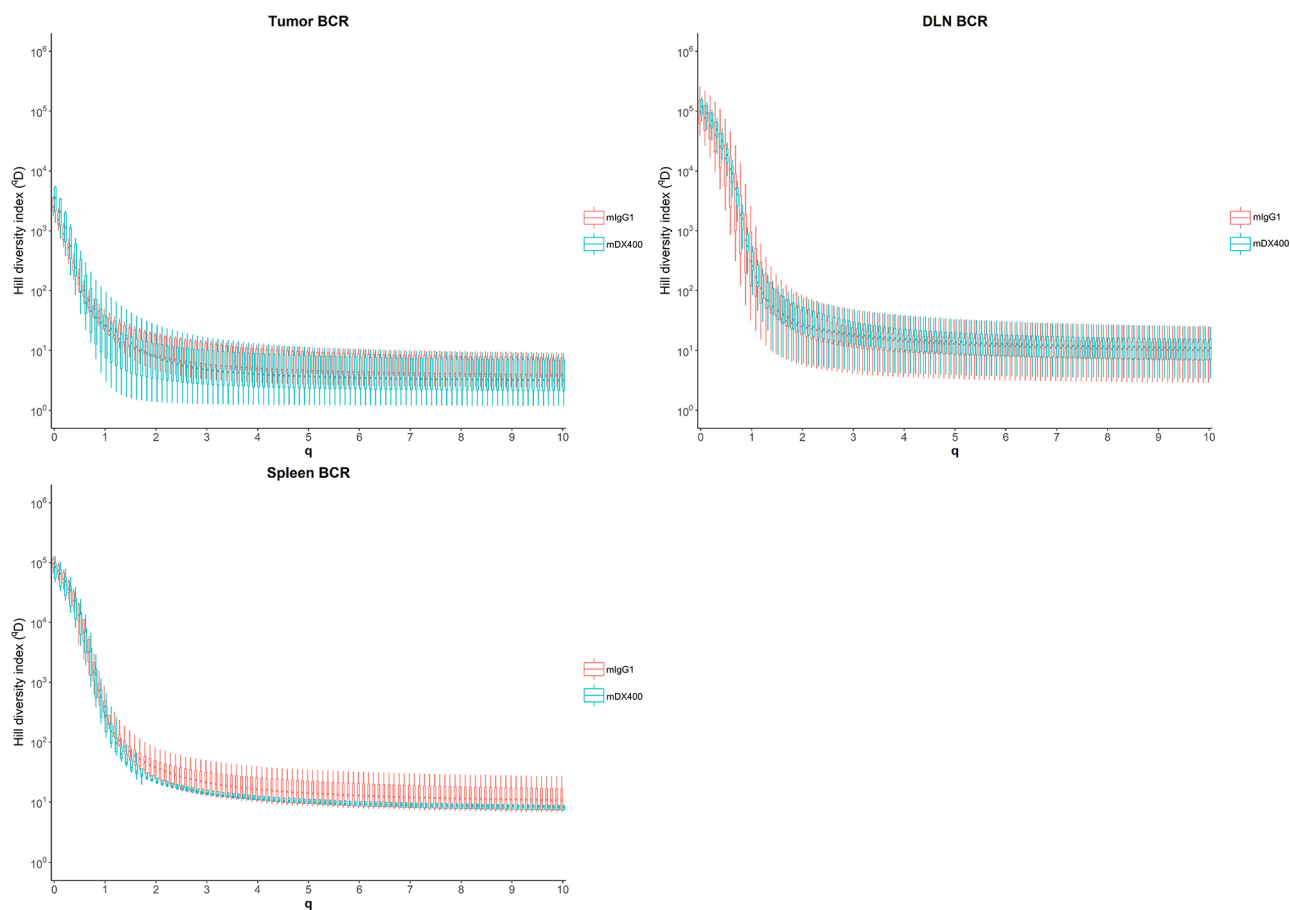


Figure S8. Diversity of BCR repertoires in tumor samples is lower than that in spleen and DLN samples. For each plot, all samples were included irrespective of treatments. The q values ranging from 0 to 10 in 0.1 increments are shown on the plot. For each q, the Hill index value is significantly (FDR <0.01) lower in tumor samples compared with spleen samples (left) or DLN samples (right). The FDR values are not shown on the plot. BCR, B cell receptor; DLN, tumor draining lymph node.

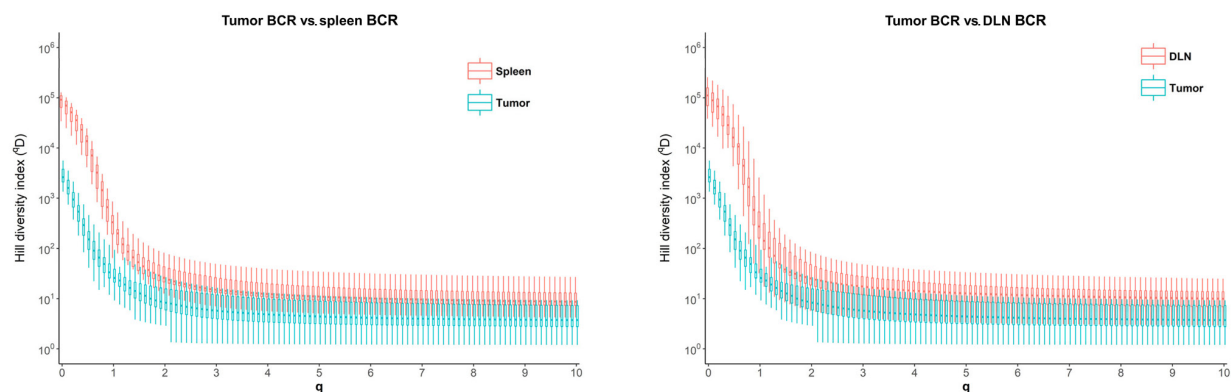




Figure S9. Sharing of the most frequent intratumoral BCR clonotypes across other tissues. The plot depicts the sharing of the top 10 (marked with violet bars on the left side) and the top 11-100 (marked with green bars on the left side) most frequent intratumoral BCR clonotypes with DLN only, spleen only, and both DLN and spleen. mDX400-treated mice are represented by blue bars on top, while mIgG1-treated mice are represented by red bars on top. The scale of the proportions of shared BCR clonotypes are shown in the color key. BCR, B cell receptor; DLN, tumor draining lymph node; mDX400, murine anti-PD-1; mIgG1, murine immunoglobulin G1.

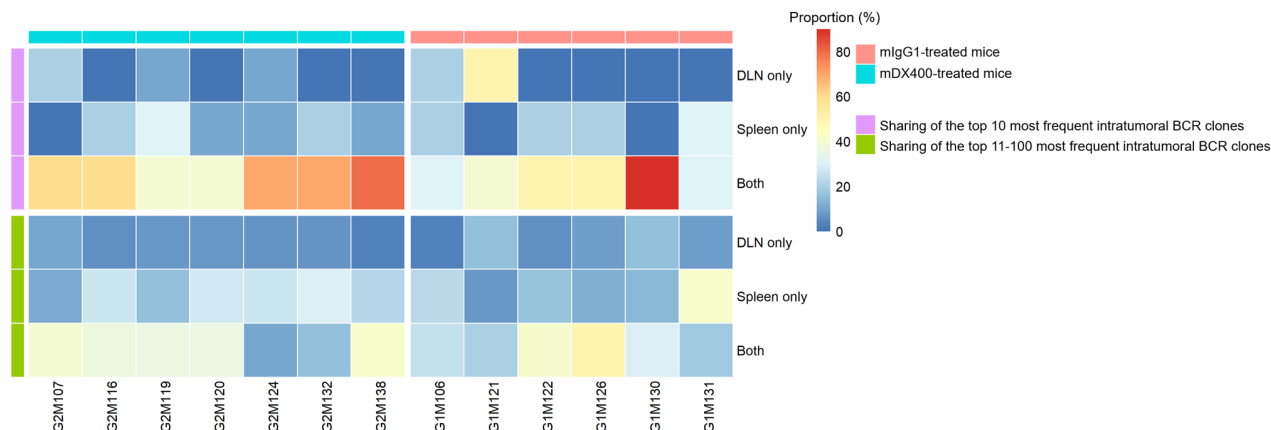


Figure S10. Mutation rates of immunoglobulin heavy chain repertoires in mDX400-group tumors where the B cell receptor clonal family is expanded and unexpanded. Mutation rates are represented by the number of mutant bases per  $10^4$  base pairs within CDR2 and FWR3, separately and together. Data are represented as the mean  $\pm$  standard deviation. \* $P < 0.05$ . mDX400, murine anti-PD-1; CDR2, complementarity determining region 2; FWR3, framework region 3.

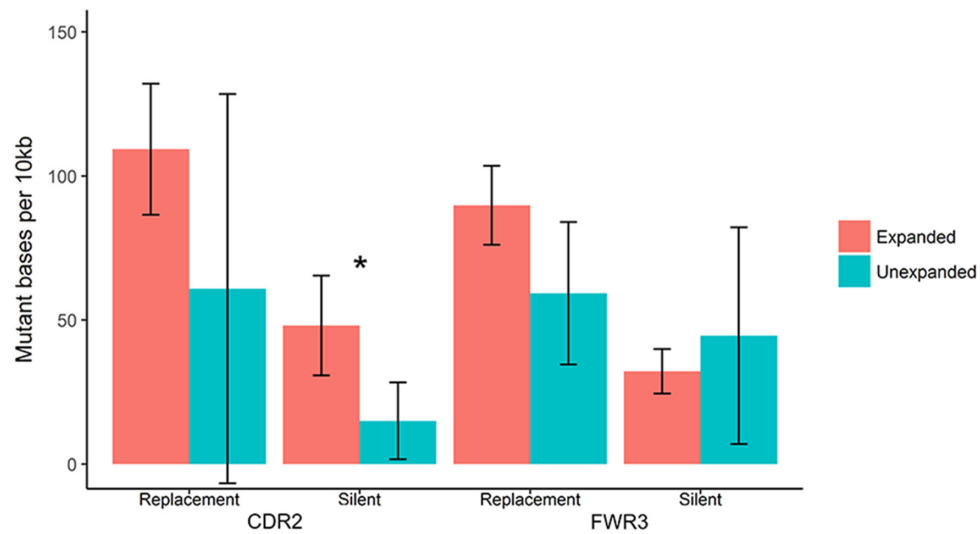


Figure S11. Lineage tree plots of IgH variable region sequences of a BCR clonal family. The BCR clonal family was highly expanded in four mDX400-group tumor samples: G2M107, G2M138, G2M119 and G2M124. For each sample, the top 50 most frequent IgH variable region sequences were used to create the plot. In each tree plot each node represents a unique IgH variable region sequence with germline sequence shown in green solid square and other sequences shown in pink solid circles. The size of each pink node is proportional to the abundance of the sequence. The number along the edge connecting two nodes represents the number of mutations between the two sequences. IgH, immunoglobulin heavy chain; BCR, B cell receptor; mDX400, murine anti-PD-1.

